Published in final edited form as:
Nanomedicine. 2012 April ; 8(3): 261–270. doi:10.1016/j.nano.2011.11.014.

NANOSCALE SURFACE MODIFICATION FAVORS BENIGN BIOFILM FORMATION AND IMPEDES ADHERENCE BY PATHOGENS

Barbara W. Trautner, Ph.D, M.D.[a,b,c,*], **Analette I. Lopez, B.S.**[d], **Amit Kumar, Ph.D**[d], **Danish M. Siddiq, M.D.**[b], **Kershena S. Liao, B.A.**[b], **Yan Li, Ph.D**[d], **David J. Tweardy, M.D.**[b,e], and **Chengzhi Cai, Ph.D**[d,*]

[a]Houston Center for Quality of Care & Utilization Studies; Michael E. DeBakey Veterans Affairs Medical Center

[b]Section of Infectious Diseases, Department of Medicine, Baylor College of Medicine, Houston, TX 77030

[c]Department of Molecular Virology and Microbiology, Baylor College of Medicine, Houston, TX 77030

[d]Department of Chemistry, University of Houston, Houston, TX 77204

[e]Department of Molecular and Cellular Biology, Baylor College of Medicine, Houston, TX 77030

Abstract

We have found in vitro that a biofilm of benign *Escherichia coli* 83972 interferes with urinary catheter colonization by pathogens, and in human studies *E. coli* 83972-coated urinary catheters are associated with lower rates of catheter-associated urinary tract infections. We hypothesized that modifying surfaces to present mannose ligands for the type 1 fimbriae of *E. coli* would promote formation of dense *E. coli* 83972 biofilms, thereby interfering with surface colonizaion by *Enterococcus faecalis*, a common uropathogen. We covalently immobilized mannose on silicon substrates by attaching amino-terminated mannose derivative to carboxylic acid-terminated monolayers *via* amidation. Fluorescence microscopy showed that *E. coli* 83972 adherence to mannose-modified surfaces increased 4.4-fold compared to unmodified silicon surfaces. Pre-exposing mannose-modified surfaces to *E. coli* 83972 established a protective biofilm that reduced *E. faecalis* adherence by 83-fold. Mannose-fimbrial interactions were essential for the improved *E. coli* 83927 adherence and interference effects.

Keywords

Escherichia coli; *Enterococcus faecalis*; adherence; biofilm; monolayer

[*]Corresponding authors. Trautner Tel.: 713 798 4264; Fax: 713 798 8948; trautner@bcm.edu, Cai Tel.: 713 794 2710; Fax: 713 743 2709; cai@uh.edu.

There is no conflict of interest for any of the authors.

BACKGROUND

Catheter-associated urinary tract infection (CAUTI) is a major health care issue without an effective preventive strategy. CAUTI is the most common nosocomial infection in the United States and is the second most common source of nosocomial bacteremia (1). Individuals who require long-term urinary catheters are chronically colonized with high levels of pathogenic bacteria (2) and thus have pathogenic biofilms on their indwelling urinary catheters. Standard antimicrobial approaches are ineffective at preventing CAUTI in chronically-catheterized individuals and lead mainly to the emergence of resistant flora (3–5). The role of biofilm in the pathogenesis of CAUTI accounts for the failure of many preventive strategies (6). Once a biofilm has formed, organisms in the biofilm are relatively protected from antimicrobials, host defenses, and shear forces (7).

Although the living tissue of the bladder wall has intrinsic defenses to deter bacterial adherence and biofilm formation (8), the catheter surface is relatively inert. Urinary catheter surface modification in terms of texture, coating, or antiseptic impregnation has been ineffective at preventing catheter colonization by pathogens and subsequent bacteriuria with long-term catheter use (9–12). Defenses that are incorporated into the catheter, such as antimicrobial agents, leach out or are consumed over time, leaving the catheter vulnerable to the constant influx of organisms from the urogenital flora.

Since biofilm formation in the catheterized urinary tract is inevitable, we are studying a new strategy for catheter defense consisting of a living, protective biofilm of benign bacteria (13–15). Ideally, this system will be self-renewing and will thus provide durable protection. The benign bacterial strain that we have chosen to form protective biofilms on urinary catheters is *Escherichia coli* 83972. This non-pathogenic bacterial strain was initially isolated from the bladder of an asymptomatic 12 year-old girl (16). *E. coli* 83972 is currently being used in clinical trials of CAUTI prevention both by our group and by a group of European investigators (14). Our two pilot clinical trials using urinary catheters pre-coated with a biofilm of *E. coli* 83972 in persons with neurogenic bladders showed that colonization with *E. coli* 83972 was associated with protection from symptomatic CAUTI (13, 15). However, in these studies, loss of *E. coli* 83972 from the bladder was accompanied by overgrowth of pathogens both on the urinary catheter and in the bladder. We anticipate that improving the surface coverage and durability of the catheter-associated benign biofilm of *E. coli* 83972 will reduce colonization and overgrowth by pathogenic bacteria, thereby improving the persistence of this protective organism in the bladder.

In vitro and in vivo we have observed that the adherence of *E. coli* 83972 to unmodified silicone urinary catheters is low in comparison to the adherence of urinary pathogens (17–19). Furthermore, we have demonstrated that we can increase adherence of *E. coli* 83972 to catheter surfaces by manipulating expression of type 1 fimbriae, and increased surface adherence leads to increased ability to block pathogen adherence to urinary catheters (17). The adhesive component of type 1 fimbriae is FimH, and its ligand is mannose (20). Therefore, we hypothesized that covalent modification of surfaces with mannose would enhance binding of *E. coli* 83972 expressing type 1 fimbriae and would promote the formation of a more dense and stable biofilm of benign *E. coli* 83972 that would block pathogen adherence. The outline of this work is depicted in Figure 1, including the preparation of the monolayers presenting mannose, adherence of *E. coli* 83972 to mannose and control surfaces, and subsequent exclusion of pathogens (*E. faecalis*) from the surface by the benign *E. coli* biofilm.

METHODS

Preparation of mannose-presenting surfaces

Hydrosilylation of 10-undecenoic acid on hydrogen-terminated silicon surfaces—Since performing experiments on silicone catheter surfaces is limited by the difficulty of characterization on the he terogeneous and curved catheter surface, we used carboxylic acid-terminated alkyl monolayers on silicon substrates as a model representing the oxidized alkyl surface of silicone urinary catheters.

Monolayers of 10-undecenoic acid were assembled on hydrogen-terminated silicon wafers by employing radical-initiated, thermal or photo-induced methods. Shards of Si (111) wafers were initially washed with ethanol and Millipore water, and treated with 5:1 (v/v) 40% NH_4F/48% HF for 30 seconds to remove native silicon oxide layer. Then, the wafers were immersed in a piranha solution (3:1 v/v concentrated H_2SO_4/30% H_2O_2) for 20 min at 90 °C. *Warning: Piranha solution is exceedingly dangerous and should be kept from organic material and handled with great caution.* The wafers were removed from the piranha solution and were thoroughly washed with Millipore water. Hydrogen-terminated silicon wafers were prepared by placing the piranha-cleaned wafers in an argon-purged 40% NH_4F solution for 10 minutes. The wafers were removed and washed quickly with degassed Millipore water and dried under a stream of argon. The hydrogen-terminated silicon wafers were immediately subjected to surface hydrosilylation with 10-undecenoic acid (**1**) using three methods (A–C in Figure 1). In method A, **1** was pressed between the hydrogen-terminated silicon wafer and a quartz window under vacuum using the setup described in our previous paper (21). A handheld 254 nm UV illuminator (EF-280C, Spectroline) was used to irradiate the surface to assemble the monolayer for 2 hours. In method B, the hydrogen-terminated silicon wafer was immersed in degassed, neat 10-undecenoic acid (**1**) in a Schlenk tube under N_2, and then heated at 160 °C for 3 hours in an oil bath. On the other hand, the hydrogen-terminated silicon wafer was immersed in a degassed mixture of **1** and 0.1 mol% of 2,2,6,6-tetramethyl-1-piperidinyloxy (TEMPO) radical initiator in method C. The monolayer assembly was performed at room temperature under N_2 for 24 hours (22–23). After each hydrosilylation, the surfaces were rinsed with boiling trifluoroacetic acid (TFA), sonicated twice in dichloromethane for 3 minutes, thoroughly washed with ethanol and dried with argon prior to characterization or coupling with mannose.

Coupling of the amino-OEG-mannose 3 to the carboxylic acid surfaces—The films presenting carboxylic acid moiety were immersed in a solution containing 50 mM of 1-ethyl-3-(3-dimethylaminopropyl) carbodiimide hydrochloride (EDC) and 30 mM of *N*-hydroxysuccinimide (NHS) in Millipore water. After 1 hour, the surfaces were removed and immediately immersed in a 3 mM solution of amino-terminated mannose **3** bearing OEG linker in Millipore water and incubated at room temperature overnight. The amino-mannose **3** was obtained from the reduction of azide-mannose **2** using triphenylphosphene (Figure 1).The surfaces were removed and washed with Millipore water followed by absolute ethanol and dried with a stream of nitrogen.

Characterization of carboxylic acid and mannose surfaces

X-ray photoelectron spectroscopy (XPS)—A PHI 5700 X-ray photoelectron spectrometer was equipped with a monochromatic Al Kα X-ray source ($h\nu$=1486.7 eV) incident at 90° relative to the axis of a hemispherical energy analyzer. The spectrometer was operated both at high and low resolutions with pass energies of 23.5 eV and 187.85 eV, respectively, a photoelectron take off angle of 45° from the surface, and an analyzer spot diameter of 1.1 mm. High-resolution spectra were obtained for photoelectrons emitted from C1s, O1s, Si 2p and N1s. All spectra were collected at room temperature with a base

pressure of 1×10^{-8} mbar. Electron binding energies were calibrated with respect to the alkyl C1s line at 284.8 eV. A PHI Multipak software (version 5.0A) was used for all data processing. The high-resolution data were analyzed first by background subtraction using the Shirley routine and a subsequent non-linear fitting to mixed Gaussian-Lorentzian functions. Atomic compositions were derived from the high-resolution scans. The ratio of the peak areas was corrected for the number of scans accumulated and for the atomic sensitivity of the element.

Ellipsometric thickness—An ellipsometer (Rudolph Research, Auto EL III), operated with a 632.8 nm He–Ne laser at an incident angle of 70°, was employed for thickness measurement of films on silicon (n = 3.839, k = 0.016), assuming a refractive index of 1.45 for the organic layers. At least three measurements were taken for each sample.

Contact-angle goniometry—Static water contact angles were measured with a KSV CAM 200 optical contact angle meter. At least three measurements were collected for each sample.

Preparation of bacterial strains

The *E. coli* 83972 derivative strains used in this study are depicted in Supplemental Figure 1. Since wild-type *E. coli* 83972 lacks a complete *fim* operon, it does not express type 1 fimbriae. Therefore, we transformed *E. coli* 83972 with pSH2, a plasmid that carries the complete *fim* operon in commercially-available pACYC184, and with pDsRed Express (Clontech), which encodes red fluorescent protein. The resulting strain of *E. coli* 83972 carrying pSH2 and pDsRed Express is called BWT38, The construction of pSH2 has been described previously (24–25). Briefly, pSH2 carries the chromosomal *fim* operon (11.2 kb) of *E. coli* J96 in the SalI site of the tetracycline resistance gene on pACYC184 (26). We have previously confirmed over expression of type 1 fimbriae by *E. coli* 83972 carrying pSH2 (17). We also created a pair of green fluorescent protein (GFP)-expressing *E. coli* 83972 derivatives with pSH2 (*fim*+) (BWT8) and without pSH2 (*fim*−) (BWT10). For the sake of clarity, we will refer to BWT38 as *fim*+ *E. coli* 83972 (red), to BWT 8 as *fim*+ *E. coli* 83972 (green), and to BWT10 as *fim*− *E. coli* 83972 (green). For the challenge pathogen, a human isolate of *Enterococcus faecalis* from a patient with bacteremia was transformed with pMV158GFP to express GFP (27).

Adherence assay of E. coli 83972 and E. faecalis

The ability of the derivative strains of *E. coli* 83972 and *E. faecalis* to adhere to mannose-modified and control surfaces was assessed by the following assay. Each wafer was placed in a 15-mL centrifuge tube containing appropriate antibiotics (20 μg/mL chloramphenicol and 100 μg/mL ampicillin for *E. coli* derivatives and 4 μg/mL tetracycline for *E. faecalis* derivatives) in Luria-Bertani (LB) broth (Difco Laboratories, Maryland) and inoculated with a starting concentration of 10^5 colony-forming units (CFU)/mL of the given strain (10 μL of a bacterial suspension with an A_{600} of 0.2 to 0.3 were added to 10 mL of LB in each tube). Wafers were incubated with *E. coli* rocking for 24 hours at 37°C. Wafers were rinsed 3 times in phosphate -buffered saline (PBS) prior to imaging. One set of experiments was done with and without 50 mM mannose in the broth to assess the role of type 1 fimbriae in the observed adherence.

Bacterial interference assay

Interference assays were performed using a modification of our established protocol for *in vitro* bacterial interference (28–29). As depicted in Supplemental Figure 2, three different types of biofilm exposures were created: sample A was exposed to *fim*+ *E. coli* 83972 alone;

sample B was exposed to *fim+ E. coli* 83972 followed by exposure to pathogenic *E. faecalis*, and sample C was exposed only to *E. faecalis*. In step 1 of the exposure sequence, samples A and B were inoculated with a starting concentration of 10^5 CFU/mL *fim+ E. coli* 83972 (also expressing DsRed) in LB media with appropriate antibiotics (20 μg/mL chloramphenicol and 100 μg/mL ampicillin), then incubated 24 hours to allow biofilm to form. Sample C (pathogen control) was incubated in sterile broth plus the same antibiotics in step 1. In step 2, all samples were transferred to separate 15-mL tubes containing sterile LB (no antibiotics). Samples B and C were then inoculated with the challenge pathogen at a starting concentration of 10^5 CFU/mL and incubated for 30 minutes, rocking, while sample A (*fim+ E. coli* 83972 control) was incubated for 30 minutes in sterile LB. In step 3, all samples were again transferred to new tubes of sterile LB and were incubated for an additional 24 hours at 37°C. After this 24-hour incubation, samples were rinsed three times in PBS then imaged using a fluorescence microscope. *E. coli* and *E. faecalis* were distinguished by red (*E. coli* 83972) or green (*E. faecalis*) fluorescence.

We performed interference tests on three surface types in parallel: on native silicon wafers without any surface modification (other than cleaning with ethanol), on carboxylic acid-terminated alkyl monolayers assembled on the silicon wafers (as an intermediate step in the mannose-attachment process), and on mannose-presenting surfaces (Supplemental Figure 2).

Fluorescence imaging of wafers

The images of bacterial adherence and interference were obtained using the 40X objective and the FITC and Cy5 wavelengths of a Nikon Eclipse E800 Microscope (Nikon Instruments, Melville, NY). A CoolSnap EZ camera (Photometrics, Tuscon, AZ) and NIS Elements software (Version 3.0, Nikon Instruments, Melville, NY) were used for image acquisition and analysis. Differentiation of the strains was based upon fluorescence emission characteristics (535 nm for GFP-expressing *E. faecalis* and 645 nm for DsRed-expressing *E. coli*). Twenty images were recorded per wafer using our standard randomization approach that avoids the wafer edges.

Testing type 1 fimbriae-mannose interaction

E. coli BWT8 (green, *fim*+) and BWT10 (green, *fim*−) were incubated overnight with native silicon, carboxylic acid, and mannose-modified surfaces in LB media with and without 50 mM mannose. A similar adherence experiment, with and without mannose, was also done with *E. coli* BWT38 (red, *fim*+). Images of adherent *E. coli* were obtained using the 40X objective of a Zeiss Axioplan II upright fluorescence microscope with a CoolSnap HQ CCD camera. GFP-expressing *E. coli* were visualized using 480/40 bandpass excitation and 535/50 bandpass emission filters and a 505 long pass dichroic beamsplitter. DsRed-expressing *E. coli* were visualized using 560/55 excitation bandpass and 645/75 emission bandpass filters and a 595 longpass dichroic beamsplitter. MetaVue (version 6.3, release 7) was used to capture the images. The biofilm on mannose surfaces was too dense to permit counting of individual bacteria, so MetaMorph software (version 6.3, release 7) was used to measure the total fluorescence intensity.

Analysis of bacterial interference results

Our measure of bacterial interference is the difference between the numbers of *E. faecalis* recovered from the pathogen control wafer (C) (*E. faecalis* alone) and from the corresponding interference wafer (B) with biofilm of *E. coli* 83972 prior to exposure to *E. faecalis*. Additionally, the comparison of the numbers of *E. faecalis* recovered from the silicon interference (B) samples and from the mannose interference (B) samples was the measure of the effect of mannose surface modification upon the ability of *E. coli* to interfere with enterococcal adherence. Since the counts of adherent organisms in the various fields

imaged per sample were not normally distributed, the median values of 10 visual fields per sample were used for further analysis. SigmaPlot for Windows 11.0 (Systat Software, Inc) was used for all analyses.

RESULTS

Preparation and characterization of mannose-presenting surfaces

As outlined in Figure 1, the COOH-terminated alkyl monolayers served as the platform for attaching mannose ligands by 3 methods: UV irradiation (A), thermal activation (B), and radical initiation (C) (22–23).

The results of X-ray photoelectron spectroscopy (XPS), static water contact angle, and ellipsometry to characterize the resulting films are summarized in Figure 2 and Supplemental Table 1. All films showed the expected XPS C1s signal at binding energies corresponding to 284.8 eV for the alkyl chains and ~289 eV for the carboxyl O-C=O groups (Figure 2A). The narrow scan Si2p spectrum showed a bulk Si peak at 99.5 eV, corresponding to the underlying, un-oxidized silicon. For the films prepared by thermal activation (Method B), a small SiO_x peak at around 102 eV also appeared (Figure 2B), indicating oxidation at the silicon interface. The films prepared by TEMPO activation (Method C) showed a small N1s peak at 399.8 eV (Figure 2C), indicating binding of some trace amounts of TEMPO during monolayer formation. Static water contact angle measurements of the films were within the range of 55°–61° (Supplemental Table 1), which was higher than what is expected for carboxylic acid surfaces. High water contact angles have been reported for COOH-terminated monolayers, including those prepared by TEMPO activated hydrosilylation, and were attributed to physisorption of trace amounts of alkyl carboxylic acids *via* strong hydrogen bonding to the surface COOH groups (30). The ellipsometric thickness of the films derived from the photo -induced hydrosilylation (Method A) was 20.8 ± 0.5 Å, much higher than the length of the adsorbate (**1**, 13.9 Å as calculated using MM2, Chem3D Ultra). This result indicated the existence of overgrowth on the monolayer, probably due to the UV-assisted decomposition of the carboxylic acid to form carbon radicals that initiate the polymerization. The thickness of the films prepared by the thermal activation (Method B) was 13.2 ± 0.5 Å, due in part to the oxide layer formed at the interface, as indicated by the Si2p peak at ~102 eV (Figure 2B). The films derived from TEMPO activation (Method C) exhibited a thickness close to the expected value (12.0 ± 0.5 Å) and the lowest water contact angles (55°). In addition, this method proved to be the most practical among Methods A–C. Therefore, we used the films prepared by this method for attaching mannose.

The mannose-amine **3** was attached to the carboxylic acid surfaces *via* amidation promoted by EDC/NHS (Figure 1). A relatively long oligo(ethylene glycol) (OEG) linker was used in **3** to increase the flexibility of the mannose ligands for binding to the FimH receptors on the *E. coli* expressing type 1 fimbriae. Upon the reaction, the thickness of the film was increased from 12.0 ± 0.3 Å to 22.4 ± 1.0 Å, while the water contact angle remained almost the same. The presence of etheric carbon atoms of the OEG-mannose is indicated by the shoulder peak at ~ 286.4 eV in the C1s XPS (Figure 2D). The small Si2p peak at 102.5 eV (Figure 2E) indicates slight oxidation at the silicon interface. The oxidation may have been facilitated by the defects due to binding of TEMPO during hydrosilylation. The presence of the N1s signal at 400.1 eV (Figure 2F), corresponding to the amide nitrogen, further confirmed the coupling of the amino-terminated mannose **3** to the carboxylic acid monolayer. The shoulder peak with a higher binding energy (402.5 eV) in the spectrum is attributed to adsorption of the NHS activating agent. Note that the common side reactions are the formation of N-acyl urea and the hydrolysis of the NHS-ester intermediate (31). The surface density of the monolayer on the precursor films was estimated to be $1.7 \pm 0.3 \times 10^{14}$ molecules/cm^2 using

the method described by Chidsey and co-workers (Supplemental Information and Supplemental Tables 2 and 3) (32). The yields of attaching mannose were estimated to be in the range of 43–74%, based on the N/C ratio measured by XPS (Supplemental Table 2). Hence, the density of mannose was estimated to be $1.1 \pm 0.2 \times 10^{14}$ molecules/cm^2.

Mannose modification of surfaces improves biofilm formation by E. coli 83972

More *fim+ E. coli* (red) were observed on the mannose-modified surfaces (Figure 3C) than on unmodified (Figure 3A) or intermediary carboxylic acid surfaces (Figure 3B). Bacterial counts of fluorescent images showed that the adherence of *E. coli* 83972 to mannose-modified surfaces (20.1×10^2 *E. coli*/field) was increased by 4.4 fold compared to adherence to unmodified silicon substrates (4.6×10^2, Figure 3D). Adherence to films presenting carboxylic acid (4.2×10^2) was not significantly different from adherence to unmodified silicon (P=0.3, T-test).

Mannose modification of surfaces improves biofilm formation by E. faecalis

We found that adherence of *E. faecalis* was also 3.4 -fold higher on mannose (7.9×10^3 enterococci/field) than on unmodified silicon surfaces (2.3×10^3, *P=0.005, T-test), as demonstrated by fluorescence microscopy images and bacterial counts. Adherence of *E. faecalis* to carboxylic acid surfaces (5.4×10^3) was intermediate between silicone and mannose, but these differences were not statistically significant (P>0.1, T-test).

E. coli 83972 biofilm impedes adherence of pathogenic E. faecalis

E. faecalis adherence on mannose surfaces without pre-existing *E. coli* biofilm served as our control (Figure 4A); a representative image of the dramatic decrease in adherence of pathogenic enterococci (green) in the presence of an interfering biofilm of benign *E. coli* (red) is shown in Figure 4B. Enterococcal adherence to mannose surfaces was reduced 83-fold by pre-exposing surfaces to *E. coli* 83972 to allow a benign biofilm to form (Figure 4C).

Surface modification improved bacterial interference

Our next question was whether *E. coli* biofilms grown on mannose-modified surfaces would better interfere with *E. faecalis* adherence than would *E. coli* biofilms formed on unmodified silicon wafers and carboxylic acid surfaces. All surfaces in Figure 5 had *E. coli* 83972 biofilms prior to exposure to enterococci; the difference is in the surface modification process. Specifically, pre-formed biofilms of *E. coli* 83972 on mannose-presenting surfaces better impeded subsequent *E. faecalis* adherence (1.4×10^2 enterococci/field, Figure 5C) than pre-formed biofilms on carboxylic acid-presenting surfaces (4.9×10^2, Figure 5B) or native silicon surfaces (10.6×10^2, Figure 5A). In pairwise comparison, the number of enterococci seen per field on mannose-presenting surfaces was significantly lower than the number seen per field on the silicon wafer. Overall, bacterial interference was improved by the presence of mannose on the films, as indicated by over 7-fold lower adherence of *E. faecalis* to the *fim+ E. coli* 83972 biofilms on the mannose-presenting substrates compared to the two other types of surfaces.

We analyzed the correlation between the number of *E. coli* and the number of *E. faecalis* from all surfaces exposed to both organisms (Supplemental Figure 3). The greater the number of adherent *E. coli*, the lower the number of *E. faecalis* that adhered to the surface (correlation coefficient −0.63, P=0.04, Spearman Rank Order).

Enhanced mannose-fimbrial interaction was required for improved adherence to mannose surfaces

We next investigated whether the observed changes in *E. coli* biofilm formation on the modified surfaces were dependent upon the interaction of type 1 fimbriae and their mannose ligands (Figure 6). The adherence of *fim+ E. coli* to all 3 surface types (Figure 6A–C) was dramatically higher than adherence of *fim−E .coli* to all 3 surface types (Figure 6D–F). Likewise, a dramatic decrease in adherence was seen on all surface types when fim+ *E. coli* were incubated with excess mannose in the media to block their fimbriae (Figure 6G–I). The increased adherence of *fim+ E. coli* 83972 over *fim−E. coli* 83972 was noted on all 3 surface types but was most marked on mannose-modified surfaces: the total fluorescence of *fim+ E. coli* was 101 times higher than the total fluorescence *fim−E. coli* to this surface type (Figure 6J). With 50mM mannose in the media (Figure 6J), the fluorescence intensity measured from *fim+ E. coli* adherent to mannose-presenting surfaces was decreased 197-fold; adherence to carboxylic acid-presenting surfaces was decreased 36-fold; adherence to native silicon surfaces was decreased 19-fold as compared to surfaces incubated in the absence of 50 mM mannose in media. Similar results were obtained for *fim+ E. coli* BWT38, which expresses DsRed instead of GFP (data not shown).

DISCUSSION

E. coli 83972 adhered in higher numbers to mannose-modified surfaces than to unmodified silicon or to intermediary carboxylic acid surfaces. *E. faecalis* exhibited the same pattern in its adherence behavior. Fortunately, a pre-existing biofilm of *E. coli* 83972 was a strong deterrent to *E. faecalis* adherence, and improving adherence of *E. coli* 83972 through covalent surface modification with mannose led to better interference with *E. faecalis* surface colonization. Both the presence of type 1 fimbriae in *fim+ E. coli* and the presence of mannose on the wafer surface were essential for this strengthened interaction.

These findings support our hypothesis that the covalent attachment of mannose to silicon surfaces enhances the formation of protective biofilms of *E. coli* 83972 that in turn effectively exclude pathogenic *E. faecalis* from adhering to the surfaces. Our results of bacterial interference on mannose-presenting monolayers refute the theoretical concern that the mannose attachment would enhance pathogenic adherence to the extent that bacterial interference would not occur. Instead, improving the interaction between benign organism and film surface effectively diminished pathogenic *E. faecalis* colonization. These results are consistent with our previous findings that increasing expression of type 1 fimbriae by *E. coli* 83972 increased adherence to urinary catheters, which in turn increased bacterial interference (17). Although the mannose-presenting surfaces increased *E. coli* 83972 adherence by 4-fold, we plan to achieve greater enhancement of the *E. coli* 83972 adherence by optimizing the mannose ligands and the linkers. We also plan to study systematically the effect of the average density versus the nanoscale local density of mannose derivatives on the binding of *E. coli* 83972.

In the clinical setting, coordinated modification of the surface and benign biofilm organism may translate to improved adherence and persistence of the benign organism in the bladder as well as increased bacterial interference. Preventing pathogens from entering the bladder through the modified catheters is the desired outcome. Enhanced interference and persistence are desirable traits for the benign biofilms that we use in our clinical trials of bacterial interference for prevention of CAUTI.

Supplementary Material

Refer to Web version on PubMed Central for supplementary material.

Acknowledgments

This study was financially supported by NIH HD058985, VA RR&D B4623, a training fellowship to AIL from the Keck Center Nanobiology Training Program of the Gulf Coast Consortia (NIH 5R90DK071054-03), and the Welch Foundation (E-1498).

Manuel Espinosa generously provided the fluorescent enterococcal plasmid, pMV158, from the Centro de Investigaciones Biológicas in Madrid.

References

1. Haley RW, Culver DH, White JW, Morgan WM, Emori TG. The nationwide nosocomial infection rate. A new need for vital statistics. American Journal of Epidemiology. 1985; 121:159–67. [PubMed: 4014113]
2. Warren JW, Tenney JH, Hoopes JM, Muncie HL, Anthony WC. A prospective microbiologic study of bacteriuria in patients with chronic ind welling urethral catheters. J Infect Dis. 1982; 146:719–23. [PubMed: 6815281]
3. Gribble M, Puterman M. Prophylaxis of urinary tract infection in persons with recent spinal cord injury: a prospective, randomized, double-blind, placebo-controlled study of trimethoprim-sulfamethoxazole. Am J Med. 1993; 95:141–52. [PubMed: 8356980]
4. Warren J, Anthony W, Hoopes J, Muncie H. Cephalexin for susceptible bacteriuria in afebrile, long-term catheterized patients. JAMA. 1982; 248:454–8. [PubMed: 7045440]
5. Summary, evidence report/technology assessment: Number 6. Agency for Health Care Policy and Research; Rockville, MD: 1999. Prevention and management of urinary tract infections in paralyzed persons. [updated January 1999; cited 2006 May 30]; Available from: http://www.ahrq.gov/clinic/epcsums/utisumm.htm
6. Ha US, Cho YH. Catheter-associated urinary tract infections: new aspects of novel urinary catheters. International Journal of Antimicrobial Agents. 2006; 28:485–90. [PubMed: 17045784]
7. Costerton J, Lewandowski S, Caldwell D, Korber D, Lappin-Scott H. Microbial biofilms. Annu Rev Microbiol. 1995; 49:711–45. [PubMed: 8561477]
8. Svanborg C, Bergsten G, Fischer H, Godaly G, Gustafsson M, Karpman D, Lundstedt AC, Ragnarsdottir B, Svensson M, Wullt B. Uropathogenic *Escherichia coli* as a model of host-parasite interaction. Curr Opin Microbiol. 2006; 9:33–9. [PubMed: 16406777]
9. Danese P. Antibiofilm approaches: prevention of catheter colonization. Chemistry & Biology. 2002; 9:873–80. [PubMed: 12204686]
10. Darouiche R, Smith J, Hanna H, Dhabuwala C, Steiner M, Babaian R, Boone T, Scardino P, Thornby J, Raad I. Efficacy of antimicrobial-impregnated bladder catheters in reducing catheter-associated bacteriuria: a prospective, randomized, multicenter clinical trial. Urology. 1999; 54:976–81. [PubMed: 10604693]
11. Jahn P, Preuss M, Kernig A, Seifert-Huhmer A, Langer G. Types of indwelling urinary catheters for long-term bladder drainage in adults. Cochrane Database Syst Rev. 2007:CD004997. [PubMed: 17636782]
12. Sofer M, Denstedt JD. Encrustation of biomaterials in the urinary tract. Curr Opin Urol. 2000; 10:563–9. [PubMed: 11148726]
13. Prasad A, Cevallos ME, Riosa S, Darouiche RO, Trautner BW. A bacterial interference strategy for prevention of UTI in persons practicing intermittent catheterization. Spinal Cord. 2009; 47:565–9. [PubMed: 19139758]
14. Sunden F, Hakansson L, Ljunggren E, Wullt B. Bacterial interference - is deliberate colonization with Escherichia coli 83972 an alternative treatment for patients with recurrent urinary tract infection? International Journal of Antimicrobial Agents. 2006; 28:S26–S9. [PubMed: 16843646]
15. Trautner BW, Hull RA, Thornby JI, Darouiche RO. Coating urinary catheters with an avirulent strain of Escherichia coli as a means to establish asymptomatic colonization. Infection Control and Hospital Epidemiology. 2007; 28:92–4. [PubMed: 17230395]

16. Andersson P, Engberg I, Lidin-Janson G, Lincoln K, Hull R, Hull S, Svanborg C. Persistence of *Escherichia coli* bacteriuria is not determined by bacterial adherence. Infect Immun. 1991; 59:2915–21. [PubMed: 1879917]

17. Trautner BW, Cevallos ME, Li H, Riosa S, Hull RA, Hull SI, Tweardy DJ, Darouiche RO. Increased expression of type-1 fimbriae by nonpathogenic *Escherichia coli* 83972 results in an increased capacity for catheter adherence and bacterial interference. J Infect Dis. 2008; 198:899–906. [PubMed: 18643750]

18. Prasad A, Cevallos ME, Riosa S, Darouiche RO, Trautner BW. A bacterial interference strategy for prevention of UTI in persons practicing intermittent catheterization. Spinal Cord. 2009; 47:565–9. [PubMed: 19139758]

19. Trautner BW, Hull RA, Thornby JI, Darouiche RO. Coating urinary catheters with an avirulent strain of Escherichia coli as a means to establish asymptomatic colonization. Infect Control Hosp Epidemiol. 2007; 28:92–4. [PubMed: 17230395]

20. Bouckaert J, Berglund J, Schembri M, De Genst E, Cools L, Wuhrer M, Hung CS, Pinkner J, Slattegard R, Zavialov A, Choudhury D, Langermann S, Hultgren SJ, Wyns L, Klemm P, Oscarson S, Knight SD, De Greve H. Receptor binding studies disclose a novel class of high-affinity inhibitors of the *Escherichia coli* FimH adhesin. Mol Microbiol. 2005; 55:441–55. [PubMed: 15659162]

21. Yam CM, Lopez-Romero JM, Gu JH, Cai CZ. Protein-resistant monolayers prepared by hydrosilylation of alpha-oligo(ethylene glycol)-omega-alkenes on hydrogen-terminated silicon (111) surfaces. Chemical Communications. 2004:2510–1. [PubMed: 15514840]

22. Perring M, Dutta S, Arafat S, Mitchell M, Kenis PJA, Bowden NB. Simple methods for the direct assembly, functionalization, and patterning of acid-terminated monolayers on Si(111). Langmuir. 2005; 21:10537–44. [PubMed: 16262318]

23. Arafat SN, Dutta S, Perring M, Mitchell M, Kenis PJA, Bowden NB. Mild methods to assemble and pattern organic monolayers on hydrogen-terminated Si(111). Chemical Communications. 2005:3198–200. [PubMed: 15968370]

24. Hull RA, Gill RE, Hsu P, Minshew BH, Falkow S. Construction and expression of recombinant plasmids encoding type 1 or D-mannose-resistant pili from a urinary tract infection *Escherichia coli* isolate. Infect Immun. 1981; 33:933–8. [PubMed: 6116675]

25. Orndorff PE, Falkow S. Organization and expression of genes responsible for type 1 piliation in *Escherichia coli*. J Bacteriol. 1984; 159:736–44. [PubMed: 6146599]

26. Chang A, Cohen S. Construction and Characterization of Multicopy Amplifiable DNA Cloning Vehicles Derived from the P15A Cryptic Miniplasmid. Journal of Bacteriology. 1978; 134:1141–56. [PubMed: 149110]

27. Nieto C, Espinosa M. Construction of the mobilizable plasmid pMV158GFP, a derivative of pMV158 that carries the gene encoding the green fluorescent protein. Plasmid. 2003; 49:281–5. [PubMed: 12749839]

28. Trautner B, Darouiche R, Hull R, Hull S, Thornby J. Pre-inoculation of urinary catheters with *Escherichia coli* 83972 inhibits catheter colonization by *Enterococcus faecalis*. J Urol. 2002; 167:375–79. [PubMed: 11743359]

29. Trautner B, Hull R, Darouiche R. *Escherichia coli* 83972 inhibits catheter adherence by a broad spectrum of uropathogens. Urology. 2003; 61:1059–62. [PubMed: 12736047]

30. Wang H, Chen SF, Li LY, Jiang SY. Improved method for the preparation of carboxylic acid and amine terminated self-assembled monolayers of alkanethiolates. Langmuir. 2005; 21:2633–6. [PubMed: 15779923]

31. Sam S, Touahir L, Andresa JS, Allongue P, Chazalviel JN, Gouget-Laemmel AC, de Villeneuve CH, Moraillon A, Ozanam F, Gabouze N, Djebbar S. Semiquantitative Study of the EDC/NHS Activation of Acid Terminal Groups at Modified Porous Silicon Surfaces. Langmuir. 26:809–14. [PubMed: 19725548]

32. Cicero R, Linford M, Chidsey C. Photoreactivity of unsaturated compounds with hydrogen-terminated silicon (111). Langmuir. 2000; 16:5688–95.

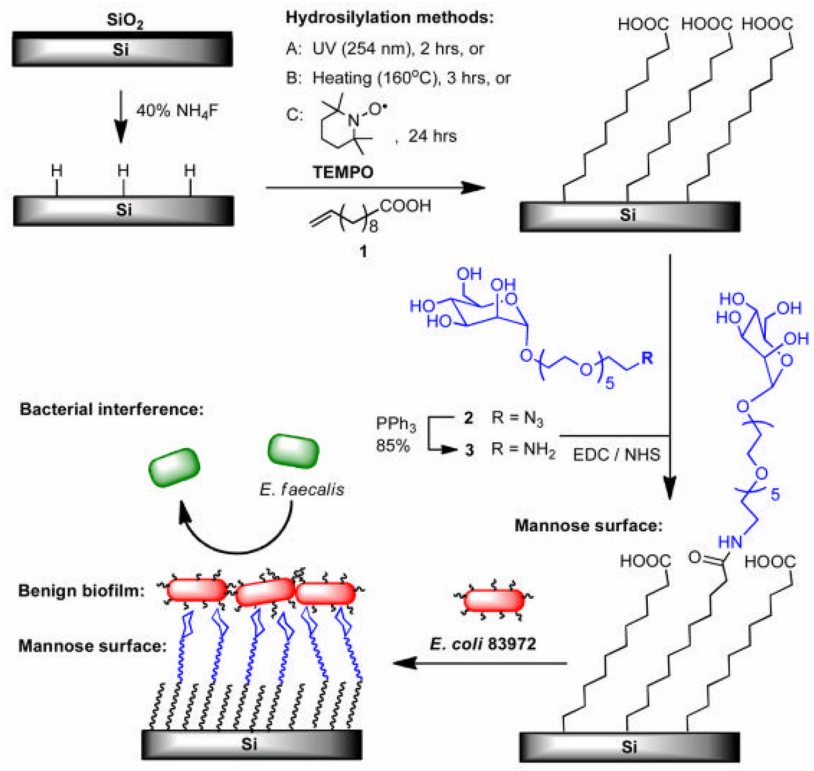

Figure 1.

Illustration of the 3 methods to prepare mannose-presenting surfaces to promote the adherence of benign *fim+ E. coli* 83972 and the subsequent exclusion of pathogenic *E. faecalis* from the surface.

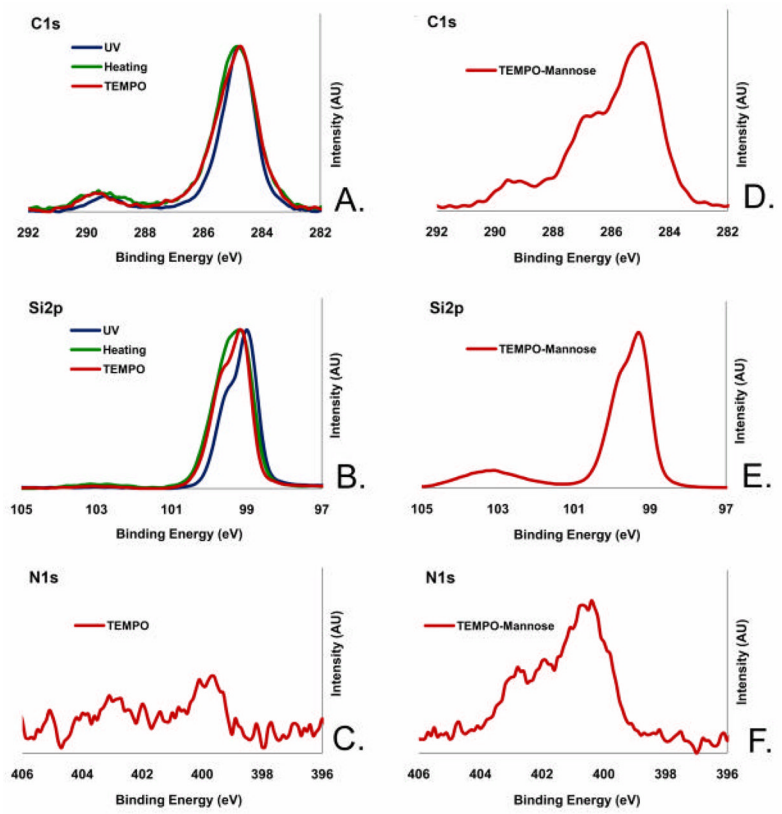

Figure 2.

XPS narrow scan in the C1s, Si2p and N1s regions for the films presenting carboxylic acid (A–C) prepared by UV irradiation (dark), and thermal activation (green) and TEMPO radical initiation (red), and the films presenting mannose (D–F) prepared by attaching amine-mannose (**3**) onto the carboxylic acid films prepared by the TEMPO activation method.

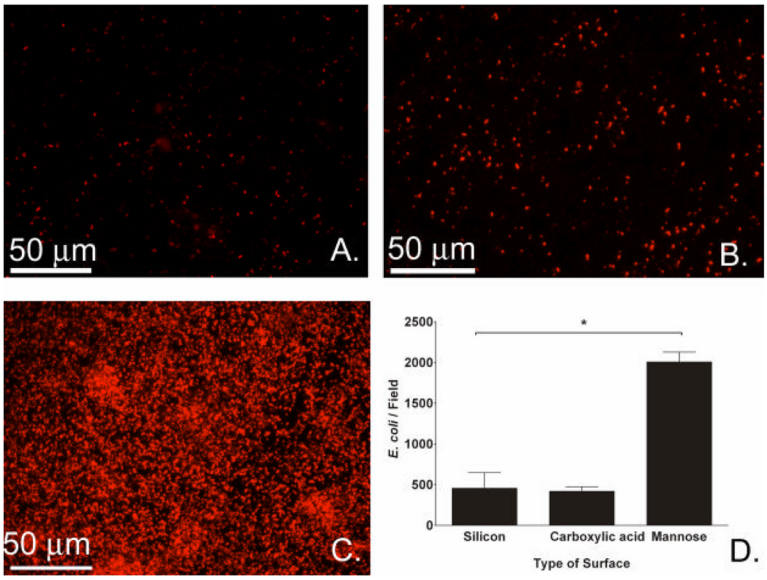

Figure 3.

Effect of surface type on adherence of *fim+ E. coli* 83972 (BWT38). Fluorescence images of *fim+ E. coli* 83972 after 24-hour incubation on silicon (A), carboxylic acid (B) and mannose surfaces (C). (D) Bacterial adherence counts obtained from the fluorescence images of the different surfaces. In each experiment, 20 fields were imaged per sample type, and the median was used for further analysis. Results are the medians of 3 experiments. (**P*<0.001 for silicon to mannose, T-test. Error bars represent 75th percentile.)

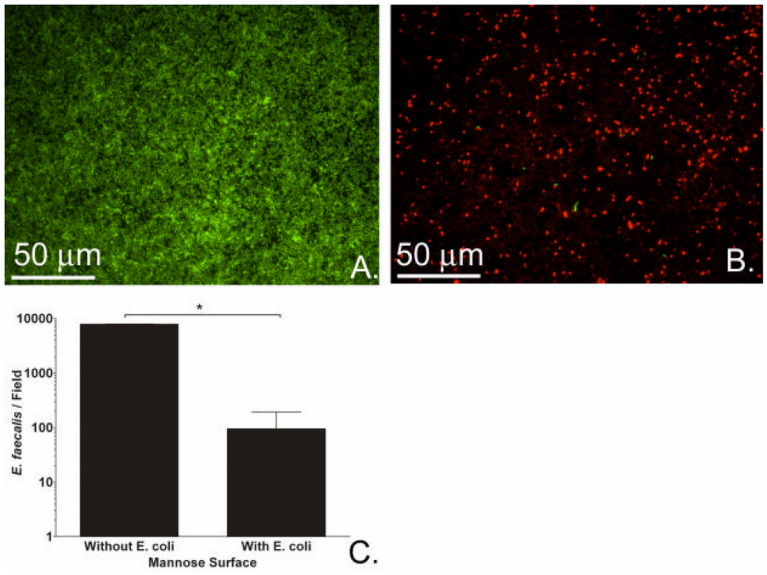

Figure 4.

Effect of pre-existing biofilm of *E. coli* on *E. faecalis* adherence. (A) Fluorescence image of *E. faecalis* (green) after 24-hour incubation (without *E. coli*) on mannose surface. (B) Fluorescence image of *E. faecalis* (green) after 24-hour incubation on mannose surfaces with pre-formed biofilm of *fim*+ *E. coli* 83972 (red). (C) Bacterial counts of *E. faecalis* grown with and without pre-formed biofilm of *E. coli* on mannose surfaces were obtained from fluorescence images. Results are the medians of 4 experiments. (**P*=0.029, Mann-Whitney Rank Sum Test. Error bars represent 75th percentile.)

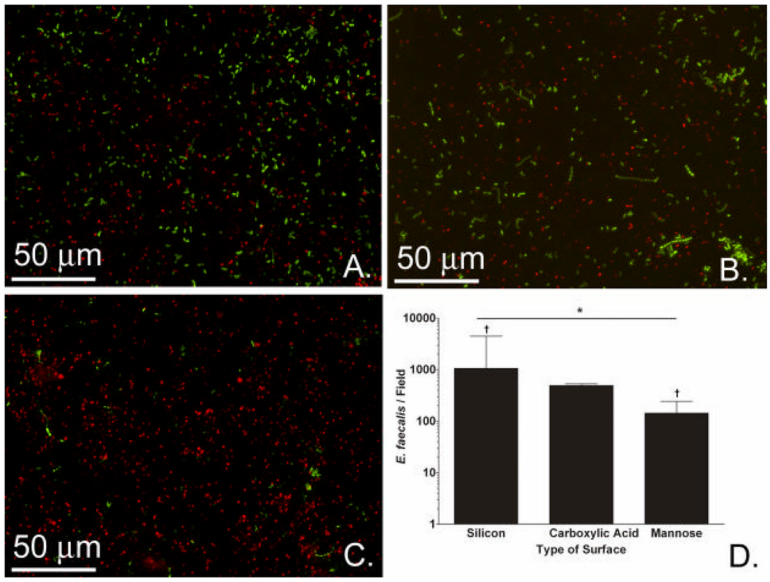

Figure 5.

Effect of surface type on bacterial interference. Fluorescence images of *E. faecalis* (green) adherent to silicon (A), carboxylic acid (B), and mannose (C) surfaces, which all had a pre-formed biofilm of *E. coli* 83972 (red). (D) Bacterial adherence counts obtained from the fluorescence images of the different surfaces (*P=0.01, N=3, Kruskal-Wallis ANOVA. †P<0.05 for silicon to mannose, Tukey Test. Error bars represent 75th percentile). Results depict the medians of 3 experiments with 20 fields imaged per sample per experiment.

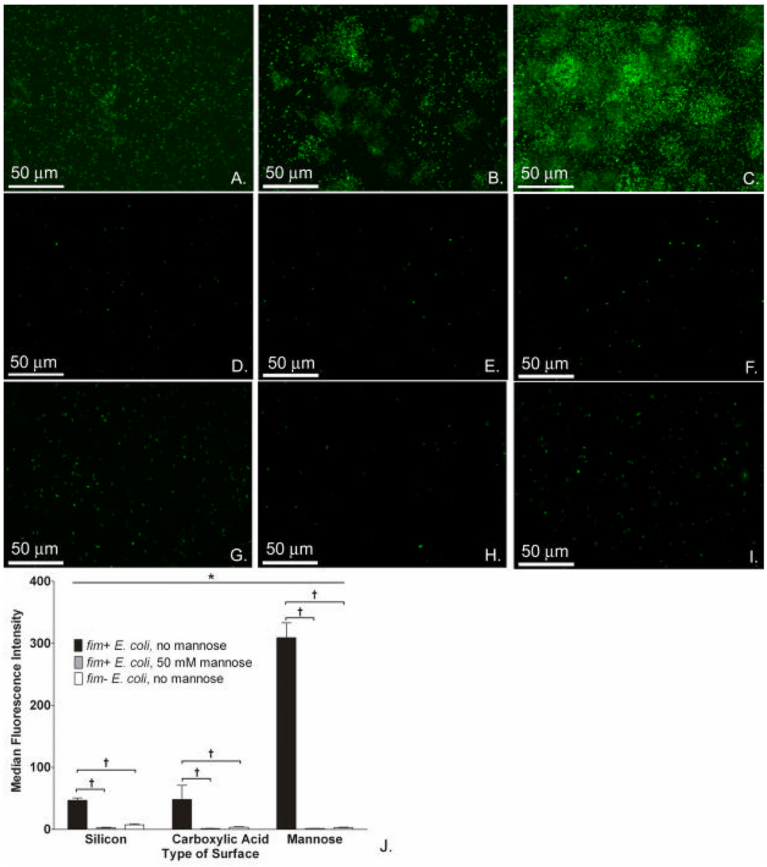

Figure 6.

Type 1 fimbriae-mannose interaction is key to enhancement of *E. coli* biofilm formation on mannose surfaces. Fluorescence images of *fim+ E. coli* 83972 (BWT8, green) on silicon (A), carboxylic acid (B), and mannose (C) surfaces in the absence of mannose in media. Fluorescence images of *fim− E. coli* 83972 (BWT10, green) on silicon (D), carboxylic acid (E), and mannose surfaces (F) in the absence of mannose in media. Fluorescence images of *fim+ E. coli* 83972 (BWT8, green) on silicon (G), carboxylic acid (H), and mannose (I) surfaces with 50 mM mannose added to growth media. (J) Adherence of *fim+ E. coli* 83972 to mannose-presenting surfaces in the absence of mannose in the media as measured by total fluorescence was significantly higher than to either the silicon or carboxylic acid-presenting surfaces (**P*<0.001, Kruskal-Wallis ANOVA).When comparing *E. coli* strains with and without *fim*, the total fluorescence intensity measured from adherent *fim+ E. coli* 83972 (BWT8) was significantly higher than that of adherent *fim− E. coli* (BWT10) on all surface types (†*P*<0.001 for pairwise comparisons, Tukey test). When comparing adherence of *fim+ E. coli* strains with and without mannose in the media, the total fluorescence intensity measured from adherent *fim+ E. coli* 83972 (BWT8) was significantly higher in the absence of mannose in the media (†*P*<0.001 for pairwise comparisons, Tukey test). Representative images of 10 fields per sample are shown, and comparisons were made on the medians of these 10 fields.